Histochem Cell Biol (2011) 135:375–387
DOI 10.1007/s00418-011-0798-y

ORIGINAL PAPER

Nicotinic acetylcholine receptor alpha7 subunit is time-dependently expressed in distinct cell types during skin wound healing in mice

Yan-Yan Fan · Tian-Shui Yu · Tao Wang · Wei-Wei Liu · Rui Zhao · Shu-Tao Zhang · Wen-Xiang Ma · Ji-Long Zheng · Da-Wei Guan

Accepted: 18 February 2011 / Published online: 10 March 2011

Abstract Recent studies have shown that nicotinic acetylcholine receptor alpha7 subunit (nAChRα7) plays an important role in regulation of inflammation, angiogenesis and keratinocyte biology, but little is known about its expression after the skin is wounded. A preliminary study on time-dependent expression and distribution of nAChRα7 was performed by immunohistochemistry, Western blotting and RT-PCR during skin wound healing in mice. After a 1-cm-long incision was made in the skin of the central dorsum, mice were killed at intervals ranging from 6 h to 14 days post-injury. In uninjured skin controls, nAChRα7 positive staining was observed in epidermis, hair follicles, sebaceous glands, vessel endothelium and resident dermal fibroblastic cells. In wounded specimens, a small number of polymorphonuclear cells, a large number of mononuclear cells (MNCs) and fibroblastic cells (FBCs) showed positive reaction for nAChRα7 in the wound zones. Simultaneously, nAChRα7 immunoreactivity was evident in endothelial-like cells of regenerated vessels and neoepidermis. By morphometric analysis, an up-regulation of nAChRα7 expression was verified at the inflammatory phase after skin injury and reached a peak at the proliferative phase of wound healing. The expression tendency was further confirmed by Western blotting and RT-PCR assay. By immunofluorescent staining for co-localization, the nAChRα7-positive MNCs and FBCs in skin wounds were identified as macrophages, fibrocytes and myofibroblasts. A number of nAChRα7-positive myofibroblasts were also CD45 positive, indicating that they originated from differentiation of fibrocytes. The results demonstrate that nAChRα7 is time-dependently expressed in distinct cell types, which may be closely involved in inflammatory response and repair process during skin wound healing.

Keywords Skin wound healing · nAChRα7 · Macrophage · Fibrocyte · Myofibroblast

Y.-Y. Fan · T.-S. Yu · T. Wang · W.-W. Liu · R. Zhao · S.-T. Zhang · W.-X. Ma · J.-L. Zheng · D.-W. Guan (✉)
Department of Forensic Pathology,
China Medical University School of Forensic Medicine,
No.92, Beier Road, Heping District, Shenyang,
Liaoning 110001, People's Republic of China
e-mail: dwguan@mail.cmu.edu.cn; dwguan007@yahoo.com.cn

Introduction

Skin wound healing consists of three phases including inflammation, proliferation and maturation, which requires an elaborate interplay among numerous cell types to orchestrate a series of regulated and overlapping events. These events include the recruitment of inflammatory cells, blood vessel formation, as well as the production of critical extracellular matrix molecules, cytokines and growth factors (Baum and Arpey 2005). Activated fibroblasts are essential for successful wound healing by transforming into myofibroblasts that secrete extracellular matrix proteins. However, their origin remains to be elucidated. A unique cell population from blood, known as fibrocytes, has been identified and characterized. There is increasing evidence that fibrocytes contribute to a population of fibroblasts and myofibroblasts that emerge in some fibrotic lesions during the repair process (Bellini and Mattoli 2007; Gomperts and Strieter 2007; Metz 2003; Andersson-Sjöland et al. 2008; Quan et al. 2004).

Neuronal nicotinic acetylcholine receptors (nAChRs) have been extensively characterized for their function in peripheral and central neurons where they play a role in modulating neurotransmission (Alkondon and Albuquerque

2004; Hogg et al. 2003). However, nAChRs are also expressed by non-neuronal cells throughout the body, indicating that they may contribute to diverse physiopathological processes such as immunomodulation and angiogenesis (Kurzen et al. 2007). Mature nAChRs are homo- or hetero-pentamers assembled with 11 genetically related, but distinct, subunits (Hogg et al. 2003). As a major nAChR subunit, nAChRα7 form homomeric pentamer of gating calcium ions (Karlin 2002), which can be activated by acetylcholine (ACh), choline and other cholinergic compounds such as nicotine. Hitherto, considerable studies have confirmed that nAChRα7 are also expressed by numerous non-neuronal cell types including astrocytes, epithelial cells, adipocytes, fibroblasts, keratinocytes and immune cells (Xiu et al. 2005; Kummer et al. 2008; Liu et al. 2004; Kurzen et al. 2007). In addition to its function in depolarization, nAChRα7 exhibits an essential role in the cholinergic anti-inflammatory pathway (Metz and Tracey 2005). Besides, nAChRα7 also mediates angiogenesis by regulating endothelial cell proliferation (Cooke 2007) and is closely involved in lipofibroblast-to-myofibroblast transdifferentiation and collagen expression (Rehan et al. 2005; Sekhon et al. 2002). These studies demonstrate that nAChRα7 function requires vagal nerve innervation as the source for ACh or nicotine exposure.

Interestingly, the skin is not innervated by parasympathetic systems, but prominently expresses distinct nAChR subunits, including nAChRα7, and releases ACh and choline by autocrine mechanisms (Klapproth et al. 1997; Kurzen et al. 2007; Misery 2004). In the skin, nAChRα7 is considerably involved in physiological and physiopathological processes. Studies demonstrate that nAChRα7 plays an important role in keratinocyte adhesion, migration, differentiation and apoptosis (Arredondo et al. 2002; Zia et al. 2000; Grando et al. 1995, Chernyavsky et al. 2004). nAChRα7 knockout mice present decreased quantity of the extracellular matrix proteins in the skin (Arredondo et al. 2003). Recent evidence also indicates that nAChRα7 activation attenuates local pro-inflammatory response to ultraviolet radiation in the skin (Osborne-Hereford et al. 2008).

The aim of this study was to characterize time-dependent expression of nAChRα7 and identify cell types expressing nAChRα7 during skin wound healing.

Materials and methods

Animal model of incised skin wound

Establishment of an animal model of incised skin wound was described previously (Guan et al. 2000). Briefly, a total of 45 8-week-old male BALB/c mice, each weighing 30–35 g, were anesthetized by intraperitoneal injection of sodium pentobarbital. A 1-cm-long incision was made with a scalpel in the skin layer on the central dorsum. After wounding, each mouse was individually housed in a cage and given sterilized chow and redistilled water to prevent bacterial infection. Specimens of 1.5 × 2 cm^2 were taken from the wounded sites after the animals were killed by cervical dislocation after anesthetization at 6 h, 12 h, 1 day, 3 days, 5 days, 7 days, 10 days and 14 days post-wounding ($n = 5$/group). The other five mice were used as controls. Each specimen was equally cut into two parts. One part was used for immunohistochemical and immunofluorescent procedure in paraffin sections and another part was used for Western blotting and RT-PCR assay, respectively.

Experiments conformed to the "Principles of Laboratory Animal Care" (National Institutes of Health published no. 85-23, revised 1985) that sought to minimize both the number of animals used and any suffering that they might experience and were performed according to the Guidelines for the Care and Use of Laboratory Animals of China Medical University.

Antibodies

The following monoclonal antibodies (mAbs) and polyclonal antibodies (pAbs) were commercially obtained: rabbit anti-nAChRα7 pAb (ab10096, Abcam, Cambridge, UK), rat anti-F4/80 mAb (sc-52664, Santa Cruz Biotechnology, CA, USA), rat anti-CD45 mAb (550539, BD Biosciences, CA, USA), mouse anti-α-SMA mAb (MS-113, Lab Vision Corporation, Fremont, CA, USA), goat anti-procollagen I pAb (sc-25974, Santa Cruz Biotechnology, CA, USA), horseradish peroxidase-conjugated goat anti-rabbit IgG (sc-2004, Santa Cruz Biotechnology, CA, USA), biotinylated donkey anti-rabbit IgG pAb (ab6801, Abcam, Cambridge, UK), Alexa Fluor® 488-labeled donkey anti-rat IgG (A-21208, Invitrogen, CA, USA), Alexa Fluor® 350-labeled donkey anti-mouse IgG (A-10035, Invitrogen, CA, USA) and Alexa Fluor® 350-labeled donkey anti-goat IgG (A-21081, Invitrogen, CA, USA). Streptavidin, Alexa Fluor® 555 conjugate (S-21381) and Hoechst33258 (H3569) were also purchased from Invitrogen.

nAChRα7 antibody specificity

Concern has been raised by recent reports suggesting that certain commercially available anti-nAChRα7 antibodies lack specificity (Herber et al. 2004; Moser et al. 2007). As the used epitopes of these antibodies mapped within the deleted region of nAChRα7-knockout (ko) mice (Fig. 1a), antibody binding produced identical labeling in wild-type

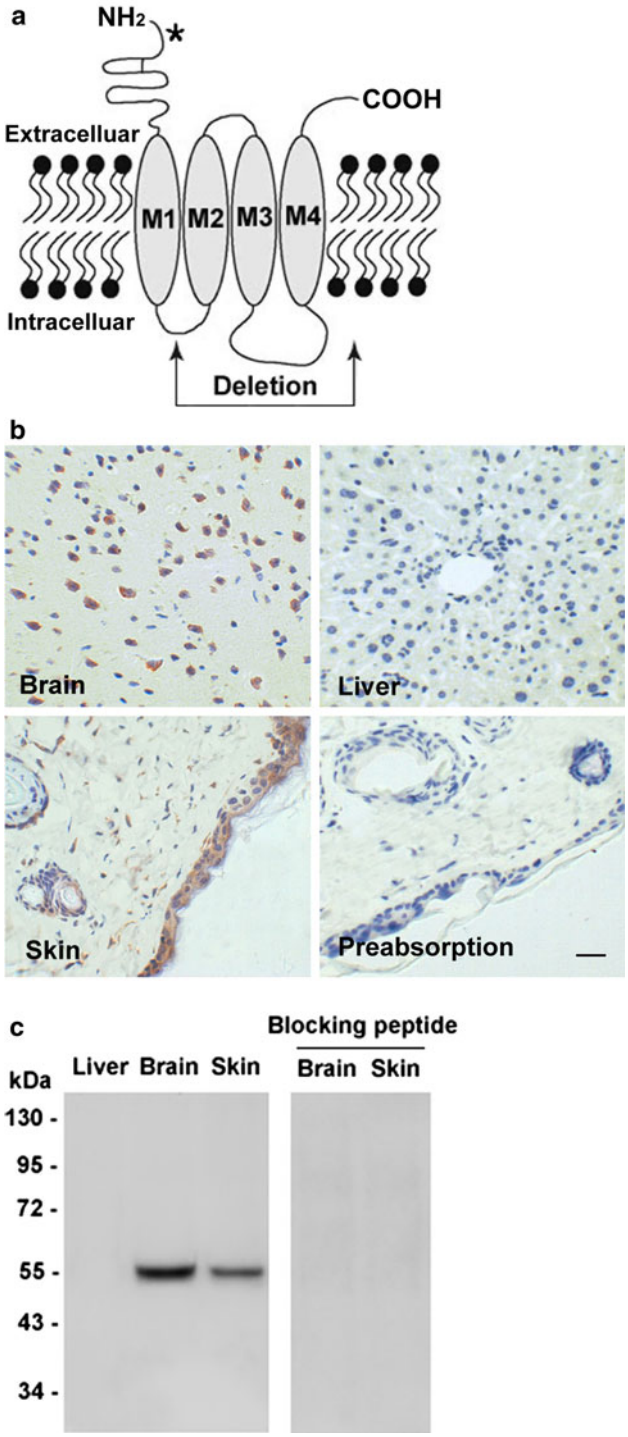

Fig. 1 **a** nAChRα7 subunit showing the extent of targeted deletion of exons 8–10 in ko mice, which encode the second, third and fourth transmembrane domains (M2, M3 and M4), the cytoplasmic loop between M3 and M4, and the short extracellular C-terminal tail (Orr-Urtreger et al. 1997). The present study employed pAb (ab10096) recognizing sequences within the distal portion of the extracellular N-terminal region of nAChRα7 subunit (denoted by *asterisk*). **b** Immunohistochemical staining of ab10096 in mouse brain, liver and skin samples. Positive staining is detected in brain and skin samples, but not in liver sample. Immunoreactivity for skin sample is blocked by preincubating corresponding peptide (ab101467, abcam, immunogen for ab10096) (*scale bar* 20 μm). **c** Analysis of nAChRα7 protein from brain, liver and skin specimens by Western blotting. A positive band at approximately 56 kDa is observed in homogenates prepared from brain and skin of mouse. This band is not observed in the liver specimen. Immunoreactive band for brain and skin specimens is removed by preincubating a blocking peptide (ab101467)

and ko mice. Although anti-nAChRα7 pAb (ab10096, Abcam, Cambridge, UK) used in the present study is not one of the questionable antibodies and has also been applied to a recent study (Mielke and Mealing 2009), it is absolutely necessary to assess the specificity of this antibody. ab10096 is a rabbit pAb prepared using a synthetic peptide derived from a proprietary sequence within residues 22–71 of the human nAChRα7 (Fig. 1a). To confirm that ab10096 specifically recognizes the sequence of nAChRα7 used in its preparation, an experiment was completed wherein the primary antibody was incubated with a commercially available blocking peptide (ab101467, the immunogen for ab10096, Abcam, Cambridge, UK) in a 1:5 ratio for 4 h at 37°C prior to use in immunohistochemistry and immunoblotting. Positive immunoreactivity of nAChRα7 was not detected after ab10096 was preabsorbed with the blocking peptide (Fig. 1b, c). To exclude the possibility that the antibody might non-specifically interact with other mouse antigens, comparative controls were made using the brain abundantly expressing nAChRα7 and the liver lacking nAChRα7 (Gahring and Rogers 2006). Strong positive reaction was seen in the brain and none was present in the liver sample (Fig. 1b, c). In addition, no positive reaction was detected in the immunohistochemical and immunoblotting procedures when the primary antibody (ab10096) was replaced by normal rabbit IgG or PBS.

Immunohistochemical staining and morphometric analysis

The skin specimens were immediately fixed wtih 4% paraformaldehyde in phosphate-buffered saline (PBS, pH 7.4) and embedded in paraffin. Serial 5-μm-thick sections were prepared. Immunostaining was performed using the streptavidin–peroxidase method. Paraffin sections were deparaffinized and rehydrated. The endogenous peroxidase was blocked by incubating the tissue sections in 3% hydrogen peroxide for 30 min at room temperature (RT) and antigen retrieval was performed with sodium citrate buffer (0.01 mol/L, pH 6.0) at 96–98°C for 10 min. Non-specific binding was blocked by incubation with normal goat serum for 2 h at RT. Afterward, the samples were

incubated with rabbit anti-nAChRα7 pAb (dilution 1:800) in a humid chamber at 4°C overnight, followed by incubation with Histostain-Plus Kit according to the manufacturer's instructions (Zymed Laboratories, South San Francisco, CA, USA). The sections were routinely counterstained with hematoxylin. As immunohistochemical controls for immunostaining procedures, some sections were incubated with normal rabbit IgG or PBS in place of the primary antibody. No false positive reaction was detected in the sections. Hematoxylin–eosin (H–E) staining was conventionally conducted.

For microscopical examination and morphometric analysis, the epidermal, dermal and subcutaneous connective tissue layers of each wound specimen, including 200 μm intact portion from the bilateral wound margins, were investigated at the light microscope level. In the present study, only polymorphonuclear cells (PMNs), mononuclear cells (MNCs) and fibroblastic cells (FBCs) were evaluated. The numbers of nAChRα7-positive cells were analyzed in ten randomly selected microscope fields in five sections of each group at a 400-fold magnification. The total number of the recruited cells or average ratio of nAChRα7-positive cells to the total cells in the ten selected microscope fields was calculated.

Double and triple indirect immunofluorescent procedure for co-localization

To identify the specific cell types that express nAChRα7, the sections were stained for nAChRα7 and the following markers: F4/80 (macrophage marker), CD45 (leukocyte marker), procollagen I (mesenchymal cell marker), α-SMA (myofibroblast marker).

A double immunofluorescent procedure was conducted to identify the expression of nAChRα7 in macrophages by a combination of anti-nAChRα7 and anti-F4/80 antibodies, as described previously (Yu et al. 2010).

For identifying the expression of nAChRα7 in fibrocytes, a triple immunofluorescent procedure was performed with anti-nAChRα7, anti-procollagen I and anti-CD45 antibodies. Briefly, deparaffinized sections were blocked with 5% BSA and incubated with rabbit anti-nAChRα7 pAb (dilution 1:500). Thereafter, the sections were incubated with biotinylated donkey anti-rabbit IgG (dilution 1:200) and streptavidin, Alexa Fluor® 555 conjugate (dilution 1:400). Then, tissue sections were further incubated with goat anti-procollagen I pAb (dilution 1:400) and rat anti-CD45 mAb (dilution 1:50) overnight at 4°C. After incubation with Alexa Fluor® 350 donkey anti-goat IgG (dilution 1:200) and Alexa Fluor® 488 donkey anti-rat IgG (dilution 1:200) at room temperature for 2 h, the sections were mounted and observed under a fluorescence microscope. The immunofluorescent images were digitally merged.

For identifying the expression of nAChRα7 in myofibroblasts, the triple immunofluorescent procedure was performed with anti-nAChRα7, anti-α-SMA and anti-CD45 antibodies. Briefly, deparaffinized sections were blocked with 5% BSA and incubated with rabbit anti-nAChRα7 pAb (dilution 1:500). Thereafter, the sections were incubated with biotinylated donkey anti-rabbit IgG (dilution 1:200) and streptavidin, Alexa Fluor® 555 conjugate (dilution 1:400). Then, endogenous IgG of mouse was blocked with Histomouse-Plus kit according to the manufacturer's instructions (Zymed Laboratories, South San Francisco, CA, USA). Tissue sections were further incubated with mouse anti-α-SMA mAb (dilution 1:200) and rat anti-CD45 mAb (dilution 1:50) overnight at 4°C. After incubation with Alexa Fluor® 350 donkey anti-mouse IgG (dilution 1:200) and Alexa Fluor® 488 donkey anti-rat IgG (dilution 1:200) at room temperature for 2 h, the sections were mounted and observed under a fluorescence microscope. The immunofluorescent images were digitally merged.

Controls for immunofluorescent co-localization

Prior to each co-localization procedure, some sections were solely incubated with a primary antiserum against antigen F4/80, CD45, procollagen I, α-SMA or nAChRα7. Reference was later made to these "single–single" control sections to insure that the pattern of terminal labeling observed for each substance in co-localized sections was in agreement with that seen in sections incubated with only one primary antiserum. In addition, negative control sections were immunostained without the primary or secondary antibody, which was replaced with normal IgG from the same species or PBS. No different staining pattern was detected in "single–single" control. No false positive reaction or cross reaction was observed in the negative control sections.

In "single–single" control, anti-procollagen I pAb (sc-25974, Santa Cruz Biotechnology) produced a predominant staining in the cytoplasm rather than in the extracellular matrix (Fig. 2a). As shown in a recent study, the intracellular staining pattern was also observed in activated hepatic stellate cells (HSC) using this antibody (Bandapalli et al. 2006). sc-25974 is a goat pAb raised against a peptide mapping near the C-terminus of the chain of collagen type I α1 precursor of human origin. To confirm its specificity, sc-25974 was pre-absorbed with a blocking peptide (sc-25974P, Santa Cruz Biotechnology). No positive reaction was detected in the pre-absorption control (Fig. 2b).

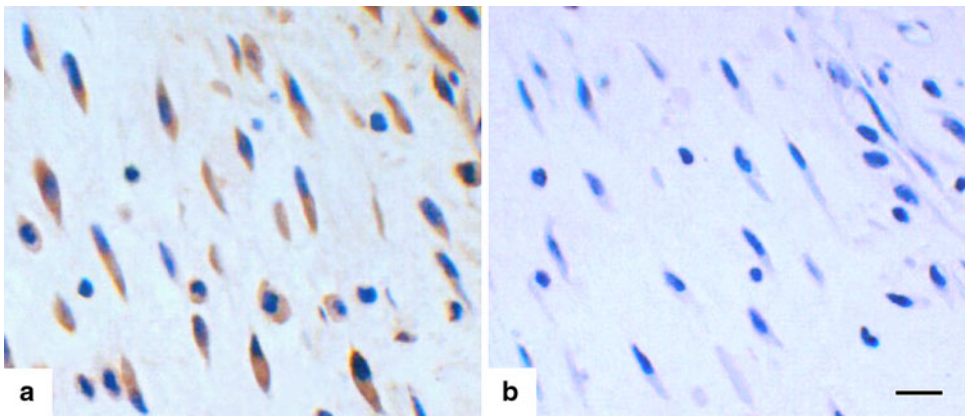

Fig. 2 Immunohistochemical staining of sc-25974 in skin wound of mouse at 7 days after injury. **a** Immunoreactivity of sc-25974 is predominantly observed in the cytoplasm. **b** Positive staining of sc-25974 is removed with an excess of blocking peptide (sc-25974p, Santa Cruz, immunogen for sc-25974) (*scale bar* 10 μm)

Table 1 Primer sequences used for reverse transcription polymerase chain reaction

Gene	Primer	Position	Product size (bp)
nAChRα7	Forward: 5′-GCA CCT CAT GCA TGG TAC AC-3′	1294–1313	241
	Reverse: 5′-GGA CAC AGC CTC CAC AAA GT-3′	1534–1515	
GAPDH	Forward: 5′-AGG CCG GTG CTG AGT ATG TC-3′	306–325	530
	Reverse: 5′-TGC CTG CTT CAC CAC CTT CT-3′	835–816	

Protein preparation and immunoblotting assay

The skin sample was cut into very small pieces using a clean razor blade and homogenized with a sonicator in RIPA buffer (sc-24948, Santa Cruz Biotechnology, CA, USA) containing protease inhibitors at 4°C. Homogenates were centrifuged at 12,000×*g* for 30 min at 4°C three times, and the resulting supernatants were collected. Protein concentration was determined by the Lowry method. Aliquots of the supernatants were diluted in an equal volume of 5× electrophoresis sample buffer and boiled for 5 min. Protein lysates (40 μg) were separated on a 12% sodium dodecyl sulfate (SDS)-polyacrylamide electrophoresis gel and transferred onto polyvinylidene fluoride (PVDF) membranes (Millipore, Billerica, MA, USA). After being blocked with 5% non-fat dry milk in Tris-buffered saline-Tween at room temperature for 2 h, the membranes were incubated with rabbit anti-nAChRα7 pAb (dilution 1:1,000) at 4°C overnight and horseradish peroxidase-conjugated goat anti-rabbit IgG at 1:10,000 dilution at 4°C overnight. The blots were visualized with Western blotting luminol reagent (sc-2048, Santa Cruz Biotechnology, CA, USA) by Electrophoresis Gel Imaging Analysis System (MF-ChemiBIS 3.2, DNR Bio-Imaging Systems, ISR). Subsequently, densitometric analyses of the bands were semi-quantitatively conducted using Scion Image Software (Scion Corporation, Maryland, USA). The relative protein levels were calculated by comparison with the amount of GAPDH (# G13-61 M, Signalchem, Canada) as a loading control.

Total RNA extraction and reverse transcription PCR

The skin specimens were immediately removed after the mice were killed, snap-frozen in liquid nitrogen and stored at −80°C. Total RNA was isolated from each specimen using RNAiso Plus (9108, Takara Biotechnology, Shiga, Japan) according to the manufacturer's instruction. The RNA pellet was air dried for 10 min and resuspended in 15 μl DEPC-treated dH_2O. Using 1 μl RNA sample, cDNA synthesis was performed in a 9 μl reaction mixture containing 2 μl $MgCl_2$, 1 μl 10× RT buffer, 3.75 μl RNase-free dH_2O, 1 μl dNTP mixture, 0.25 μl RNase inhibitor, 0.5 μl avian myeloblastosis virus reverse transcriptase (AMV-RT) and 0.5 μl Random 9 mers provided by TaKaRa RNA PCR Kit (AMV) Ver.3.0 (RR019, Takara Biotechnology, Shiga, Japan). The resulting cDNA was used for PCR with the sequence-specific primer pairs for nAChRα7 and GAPDH. PCR amplification was performed in a 60 μl reaction mixture which contained 12.5 μl 5× PCR Buffer, 36 μl sterile H_2O, 0.5 μl *TaKaRa Ex Taq*, 0.5 μl forward primer, 0.5 μl reverse primer and 10 μl cDNA. The amplified PCR products were identified using electrophoresis of 6 μl aliquots on a 2% agarose gel and were stained with Genefinder (204001, Bio-V, Xiamen, China). To exclude any potential genomic DNA contamination, each PCR was also performed without the

RT step. No DNA amplification product was detected. All PCRs were repeated at least three times for each cDNA. For normalization of the amount of different cDNAs, GAPDH was used as an internal standard. The specific primers of nAChRα7 and GAPDH are shown in Table 1.

The products were visualized with Electrophoresis Gel Imaging Analysis System (ChemiImager 5500, Alpha Innotech, USA). Labworks Image Acquisition and Analysis Software (UVP Inc., Upland, CA, USA) were employed for semi-quantitative digital image analysis of the PCR product bands. The ratios of nAChRα7 to GAPDH band intensity were calculated to normalize the determined values.

Statistical analysis

Data were expressed as mean ± standard deviation (SD) and analyzed using SPSS for Windows 11.0. One-way ANOVA was used for data analysis between two groups. The difference associated with $P < 0.05$ was considered to be statistically significant.

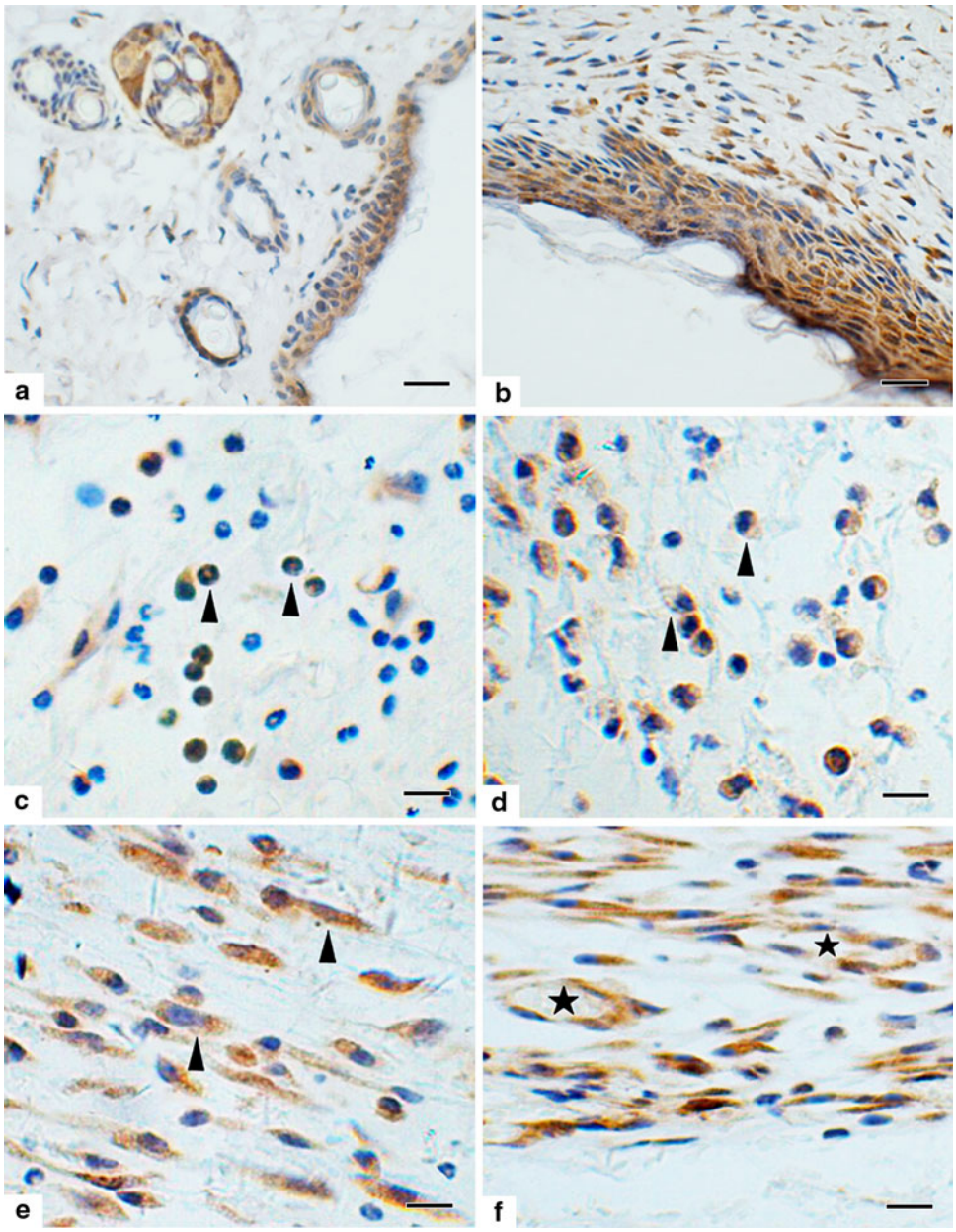

Fig. 3 Immunohistochemical staining of nAChRα7 in mouse skin samples. **a**, **b** The expression of nAChRα7 is detected in normal mouse skin and in the neoepidermis of skin wounds at 10 days after injury. **c** nAChRα7 immunoreactivity is found in a few PMNs (*arrowheads*) at 12 h post-injury. **d** The infiltrating MNCs (*arrowheads*) reveal nAChRα7-positive staining at 3 days post-injury. **e**, **f** FBCs (*arrowheads*) and endothelial-like cells of regenerated vessels (*asterisks* represent vessel) are positively immunostained with antibody against nAChRα7 in the wounded area at 7 days post-injury (*scale bar* in **a** and **b** = 20 μm; in **c**–**f** = 10 μm)

Results

Histological examination, immunohistochemical staining and morphometric analysis for nAChRα7-positive cells

In H–E-stained sections, polymorphonulcear cells (PMNs) appeared at the margin and peripheral zone of the wounds at 6 h post-wounding and obviously increased in number at 12 h. A large number of mononuclear cells (MNCs) accumulated in the margin of the wounds at 1 day post-wounding and peaked at 3 days. From 3 days post-wounding, fibroblastic cells (FBCs) were present at the bottom of the wound cavity, markedly augmented in number at 5 days, and peaked at 7 days. During this period of time, angiogenesis and newly formed granulation tissue were also observed. Simultaneously, the epidermal cells proliferated from monolayer to multiple layers and completely covered the wound. After 10 days post-wounding, the total number of cells and the density of regenerated vessels in the wound zones started to decrease and granulation tissue gradually transformed into scar tissue.

In uninjured skin specimens, nAChRα7-positive staining was observed in epidermis, hair follicles, sebaceous glands, vessel endothelium and resident dermal FBCs (Fig. 3a). In wounded specimens, a small number of PMNs and MNCs showed nAChRα7 immunoreactivity from 6 to 12 h (Fig. 3c). At 1 and 3 days, a large number of MNCs were positively immunostained with anti-nAChRα7 antibody (Fig. 3d). From 5 days post-wounding, nAChRα7 immunoreactivity was mainly detected in FBCs (Fig. 3e). At 14 days after injury, there were still a small number of MNCs and a number of FBCs labeled with anti-nAChRα7 antibody. In addition, nAChRα7-positive staining was also clearly present in endothelial-like cells of regenerated vessels (Fig. 3f) and neoepidermis (Fig. 3b) from 5 to 14 days post-wounding.

Figure 4 represents the number of total cells and nAChRα7-positive cells in relation to wound age. The mean values of the nAChRα7-positive ratios are shown in Table 2. In general, the positive ratios were relatively low in groups from 6 to 12 h post-wounding, while a significant increase in the positive ratios was observed in groups from 1 to 14 days post-wounding as compared to that of control ($P < 0.05$).

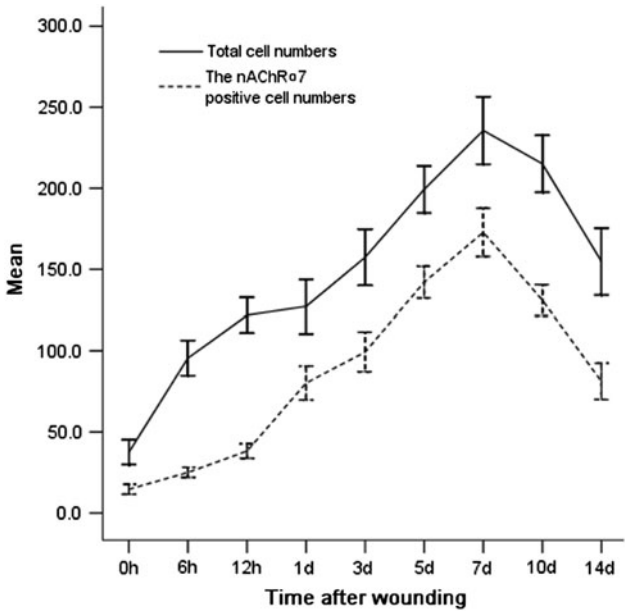

Fig. 4 The time-dependent changes of the number of total cells and nAChRα7-positive cells. Representative results from five individual animals are shown. The data at 0 h after incision represent the results obtained from normal mice as control group. Note that two variables reached peak levels at 7 days after injury

Cellular localization of nAChRα7 using immunofluorescent staining

By double immunofluorescent staining, the majority of nAChRα7$^+$ MNCs were found to express macrophage marker (F4/80). At 1 and 3 days after injury, a great quantity of nAChRα7$^+$ macrophages accumulated in the margin of the wounds (Fig. 5). With extension of wound age, less nAChRα7$^+$ macrophages were detectable at the wound site.

By triple immunofluorescent procedure, the expression of nAChRα7 in fibrocytes or myofibroblasts was identified. From 6 h to 1 day post-wounding, a large number of CD45$^+$ cells infiltrated into the margin of the wounds, which showed a negative staining for procollagen I or α-SMA (Figs. 6d, 7d). From 3 days post-wounding,

Table 2 The positive ratios of nAChRα7 in each wound group

Group	*n*	Mean ± SD (%)
0 h	5	38.70 ± 1.40
6 h	5	26.15 ± 1.31[a]
12 h	5	31.41 ± 2.76[b]
1 day	5	63.13 ± 3.68[b]
3 days	5	63.24 ± 4.39[a]
5 days	5	71.48 ± 5.10[b]
7 days	5	73.57 ± 6.16[a]
10 days	5	60.98 ± 3.50[b]
14 days	5	52.65 ± 3.24[b]

The data at 0 h represent the results obtained from normal mice as control group

[a] $P < 0.05$ (vs. control group)

[b] $P < 0.05$ (vs. control group and preceding group)

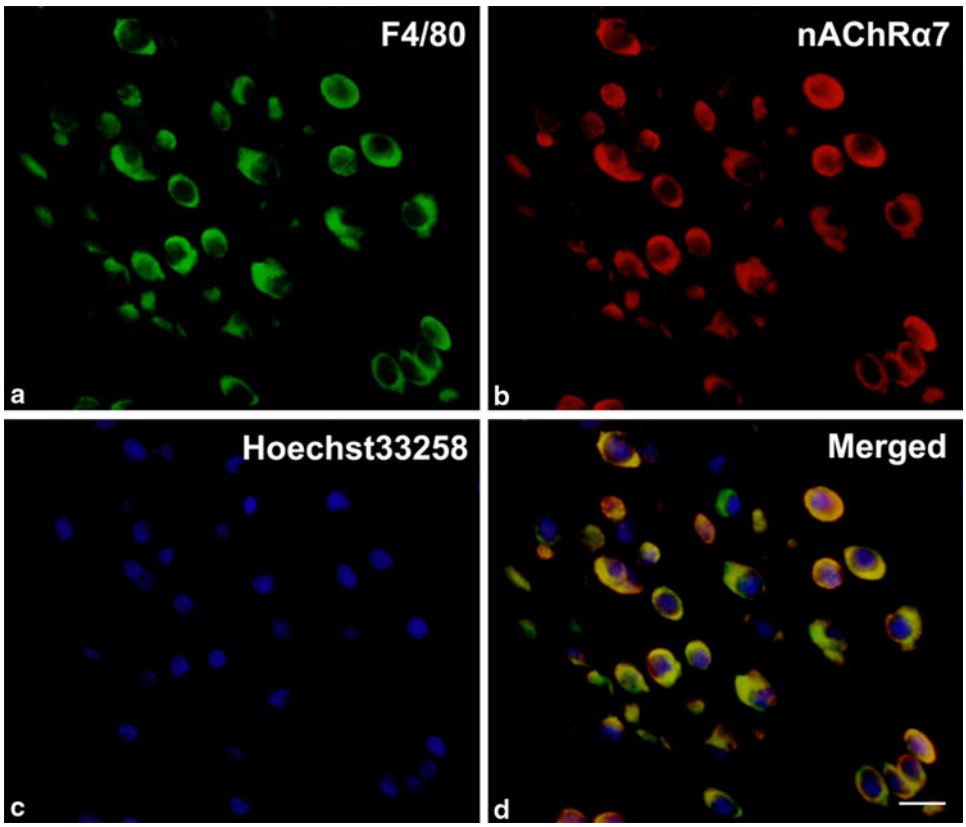

Fig. 5 Double immunofluorescence analysis was performed to determine nAChRα7-expressing macrophages at 3 days post-injury. The samples were immunostained with anti-F4/80 (**a**, *green*) and anti-nAChRα7 (**b**, *red*). Nuclei were counterstained with Hoechst33258 (**c**, *blue*). Signals in **a**–**c** were digitally merged in **d**. The nAChRα7$^+$/F4/80$^+$ cells presented as *yellow* signals in the merged image. Representative results from three independent experiments are shown here (*scale bar* 10 μm)

CD45$^+$/procollagen I$^+$ cells, i.e., fibrocytes, were detected in the wound site (Fig. 6h). From 5 to 14 days post-wounding, CD45$^+$/α-SMA$^+$ cells were observed in granulation tissue, indicating that these myofibroblasts originated from differentiation of the fibrocytes (Fig. 7). From 3 to 14 days post-injury, most of the fibrocytes showed a positive staining for nAChRα7 (Fig. 6). From 5 to 14 days post-wounding, a large number of CD45$^+$ myofibroblasts were also nAChRα7-positive cells (Fig. 7). In addition to the fibrocytes and CD45$^+$ myofibroblasts, a large number of CD45$^-$/procollagen I$^+$ cells or CD45$^-$/α-SMA$^+$ cells were also positively immunostained with anti-nAChRα7 antibody from 5 to 14 days post-wounding (Figs. 6, 7).

Western blotting and RT-PCR

A significant increase in the relative protein level of nAChRα7 to GAPDH was found at 1, 3, 5, 7, 10 and 14 days as compared with that of control, which maximized at 7 days post-wounding by semi-quantitative analysis ($P < 0.05$; Fig. 8a, b).

nAChRα7 mRNA could be detected in all skin samples including the control by RT-PCR. Similar to Western blotting results, a significant increase in the ratio of nAChRα7 mRNA to GAPDH mRNA was found at 1, 3, 5, 7, 10 and 14 days as compared to that of control, which peaked at 7 days post-wounding by semi-quantitative analysis ($P < 0.05$; Fig. 9a, b).

Discussion

In the present study, nAChRα7-positive staining was observed in epidermis, hair follicles, sebaceous glands, vessel endothelium and resident dermal FBCs in uninjured skin specimens. After skin injury, the number of nAChRα7-positive cells started to increase in the inflammatory phase and peaked in the proliferative phase. As wound age prolonged, nAChRα7 was temporally detected in PMNs, macrophages, fibrocytes, myofibroblasts, endothelial-like cells of regenerated vessels and neoepidermis. An up-regulated expression of nAChRα7 was demonstrated during skin wound healing. To our knowledge, this is the first report that characterized nAChRα7 expression in cells after skin injury.

During skin wound healing, there seems to be abundant endogenous agonists for nAChRα7. It has been demonstrated that keratinocytes are a significant source of ACh and can produce, store, secrete and degrade ACh (Grando

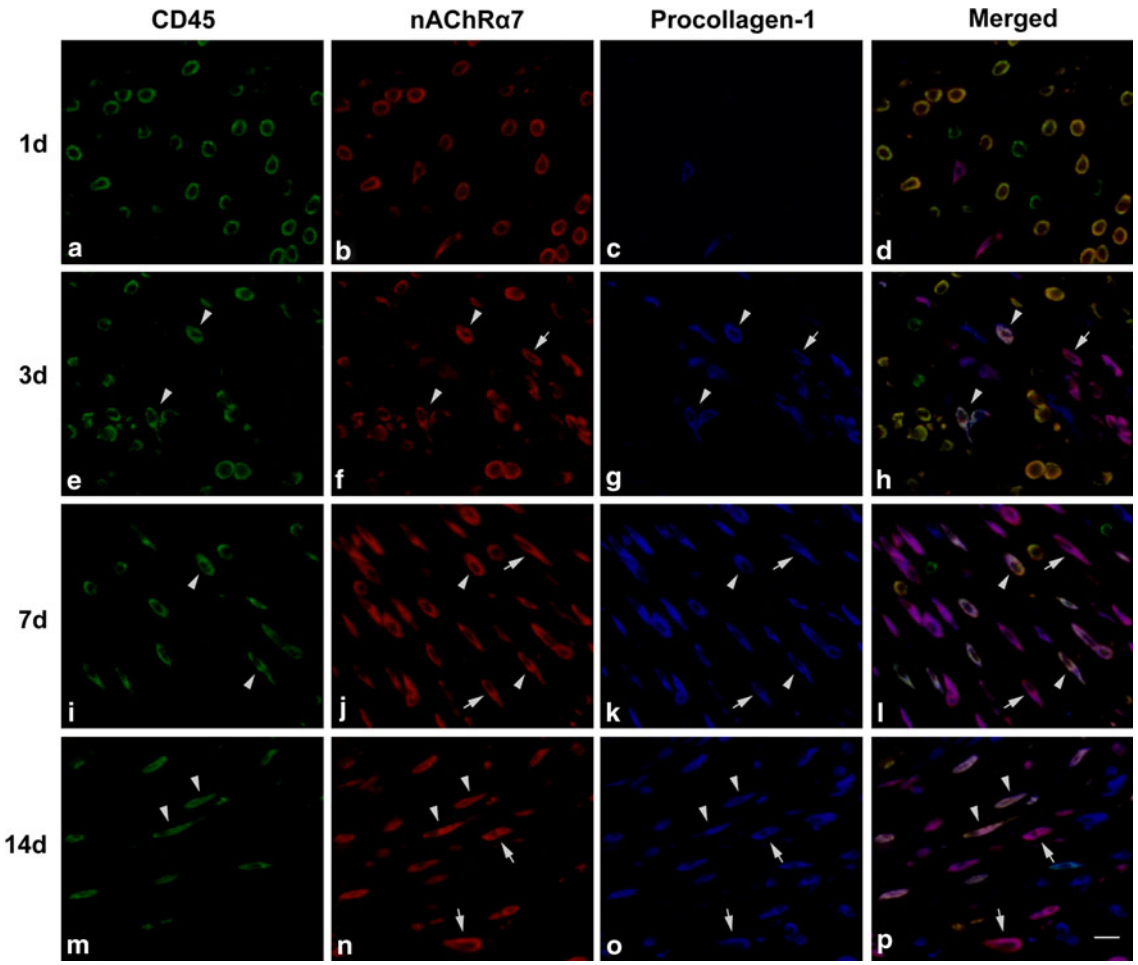

Fig. 6 Triple immunofluorescence analysis was performed to determine the expression of nAChRα7 in fibrocytes in the wounds at 1 (**a**–**d**), 3 (**e**–**h**), 7 (**i**–**l**) and 14 (**m**–**p**) days post-injury. The samples were immunostained with anti-CD45 (**a**, **e**, **i** and **m**, *green*), anti-nAChRα7 (**b**, **f**, **j** and **n**, *red*) and anti-procollagen I (**c**, **g**, **k** and **o**, *blue*). Merged signals are shown in **d**, **h**, **l** and **p**. The $CD45^+$/$nAChR\alpha7^+$/collagen I^+ cells presented *white* signals (*arrowheads*), and $CD45^-$/$nAChR\alpha7^+$/collagen I^+ cells showed *purple* signals (*arrows*) in merged images. The extracelluar matrix staining for procollagen I has not been shown in experimental dilution. Representative results from three independent experiments are shown here (*scale bar* 10 μm)

et al. 1993). ACh is degraded by acetylcholinesterase (AChE), an enzyme with high activity in the dermis, which is also strongly expressed in re-epithelializing keratinocytes after skin incision (Anderson et al. 2008). Choline as a precursor and the main degradation product of ACh is more stable and widely available and has a selective affinity to nAChRα7 (Papke et al. 1996; Alkondon et al. 1997; Grando 1997; Kurzen et al. 2007). Moreover, ACh is produced by granulocytes, macrophages and lymphocytes as well (Neumann et al. 2007; Kawashima and Fujii 2008).

The inflammatory process of wound healing is perpetuated through macrophage production of pro-inflammatory cytokines such as IL-1, IL-6 and TNF-α (Werner and Grose 2003). It is well established that activation of nAChRα7 on macrophages leads to efficient suppression of pro-inflammatory cytokine production (Tracey 2002; Wang et al. 2003; Su et al. 2007). nAChRα7 expressed by macrophages in skin wounds might play a role in mediating the effect of cholinergic anti-inflammation.

Fibrocytes are bone marrow-derived mesenchymal progenitors, which co-express leukocyte (CD45, CD34, CD13) and mesenchymal markers (type I collagen, type I procollagen, fibronectin) (Chesney et al. 1998; Bucala et al. 1994; Abe et al. 2001; Phillips et al. 2004; Moore et al. 2005; Hashimoto et al. 2004; Mori et al. 2005; Sakai et al. 2006; Schmidt et al. 2003; Aiba and Tagami 1997; Yang et al. 2005). Moreover, fibrocytes are characterized by their ability to differentiate along multiple lineages, such as myofibroblasts, osteoblasts and adipocytes, giving rise to fully differentiated cells with distinct function (Choi et al. 2010; Hong et al. 2005; Phillips et al. 2004). In skin wound healing, fibrocytes can infiltrate into the

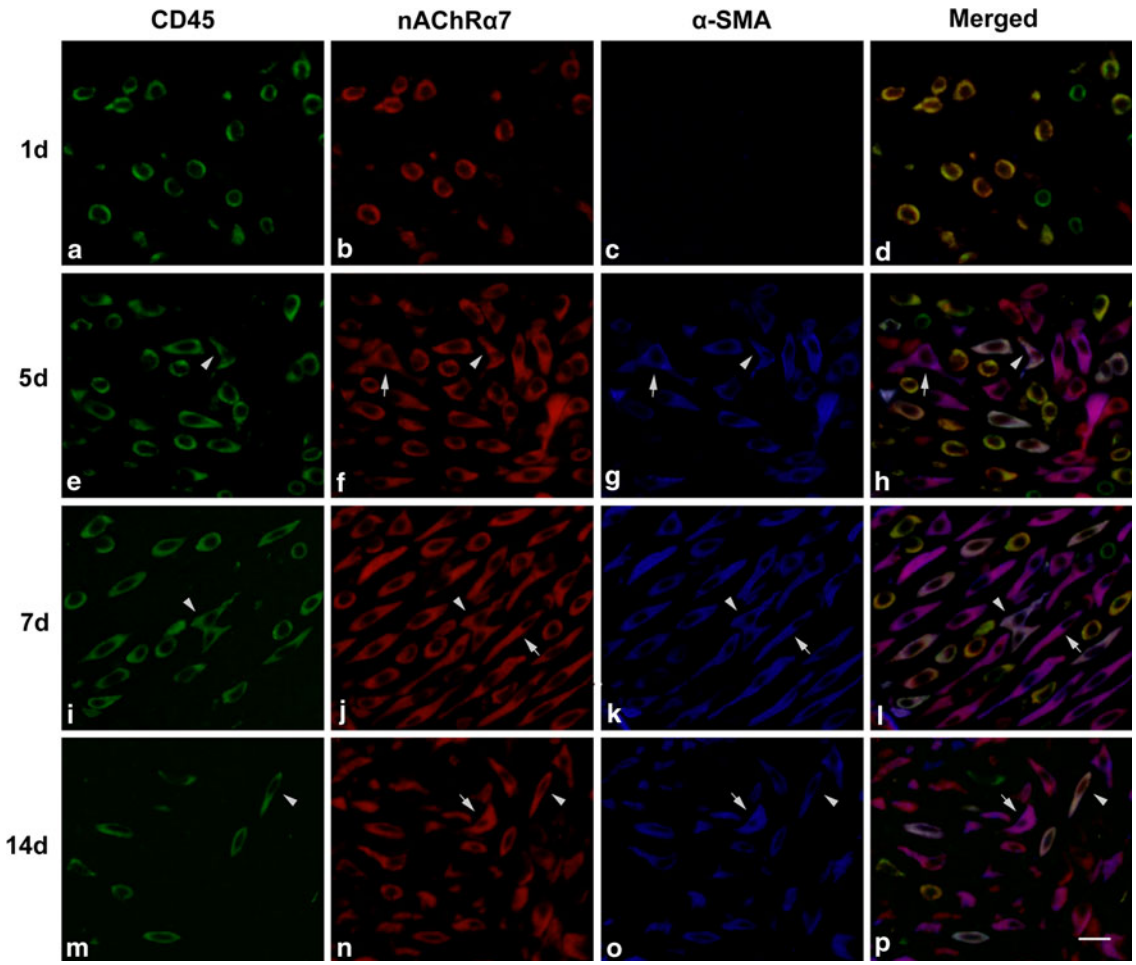

Fig. 7 Triple immunofluorescence analysis was performed to determine the expression of nAChRα7 in myofibroblasts in the wounds at 1 (**a**–**d**), 3 (**e**–**h**), 7 (**i**–**l**) and 14 (**m**–**p**) days post-injury. The samples were immunostained with anti-CD45 (**a**, **e**, **i** and **m**, *green*), anti-nAChRα7 (**b**, **f**, **j** and **n**, *red*) and anti-α-SMA (**c**, **g**, **k** and **o**, *blue*). Merged signals are shown in **d**, **h**, **l** and **p**. The $CD45^+$/$nAChR\alpha7^+$/α-SMA^+ cells presented *white* signals (*arrowheads*) and $CD45^-$/$nAChR\alpha7^+$/α-SMA^+ cells showed *purple* signals (*arrows*) in merged images. Representative results from three independent experiments are shown here (*scale bar* 10 μm)

wound site and further differentiate into myofibroblasts ($CD45^+$/α-SMA^+ cells) (Mori et al. 2005). Specific involvement of nAChRα7 is demonstrated in nicotine-induced lipofibroblast-to-myofibroblast transdifferentiation (Rehan et al. 2005). In our skin incision model, fibrocytes ($CD45^+$/procollagen I^+ cells) and myofibroblasts ($CD45^+$/α-SMA^+ cells) were also detected and both expressed nAChRα7. Our results suggest that nAChRα7 may play roles in fibrocyte-to-myofibroblast differentiation in skin wound healing.

Several researches suggest that fibrocytes progressively lose their leukocyte markers (CD45, CD34, CD13) after recruitment into specific tissues (Yang et al. 2005; Mori et al. 2005; Andersson-Sjöland et al. 2008). In the present study, we also observed that nAChRα7 was expressed by a large number of $CD45^-$/procollagen I^+ cells and $CD45^-$/α-SMA^+ cells at the proliferative phase post-wounding. These cells might originate from resident dermal fibroblasts or fibrocytes that lost their leukocyte marker.

It is known that activation of nAChRα7 leads to increased intracellular calcium. Elevated intracellular calcium can reduce collagen synthesis in fibroblasts (Flaherty and Chojkier 1986). It is proposed that chronic prenatal nicotine exposure leads to desensitization of nAChRα7, decreases intracellular calcium in fetal lung fibroblasts and therefore increases collagen production (Sekhon et al. 2002). Recent evidence also showed that myofibroblast contraction may be mediated by calcium ion influx (Follonier Castella et al. 2010). Further studies are needed to determine if nAChRα7 can additionally mediate regulation of collagen expression in fibrocytes and dermal fibroblasts or mediate myofibroblast contraction.

In addition, we also detected strong nAChRα7 expression in neoepidermis in skin wounds. Notably, the

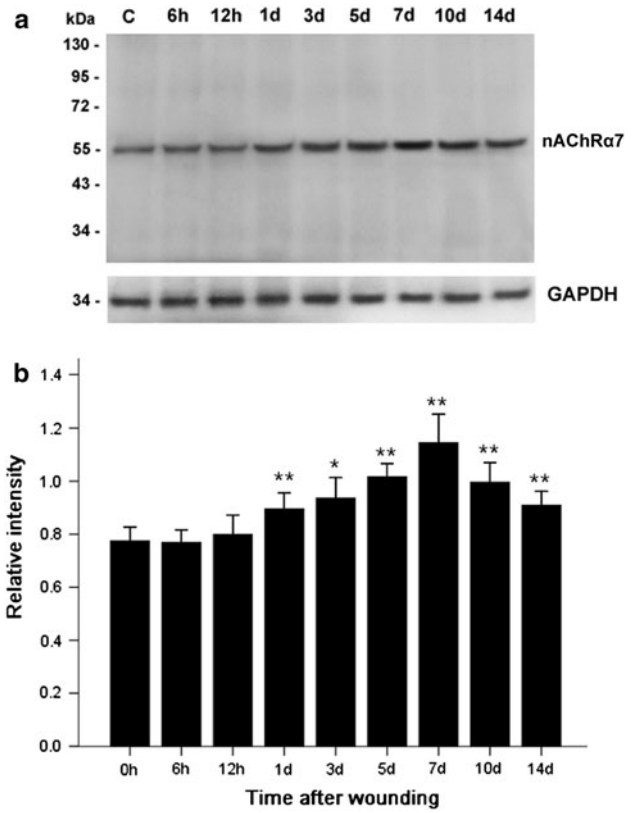

Fig. 8 **a** Analysis of nAChRα7 and GAPDH protein from skin specimens by Western blotting. *lane C* represents the result of the control skin samples. Representative results from five individual animals are shown. **b** Relative intensity of nAChRα7 to GAPDH. All values are expressed as the mean ± SD ($n = 5$). $^{**}P < 0.05$ (vs. control group and preceding group); $^{*}P < 0.05$ (vs. control group)

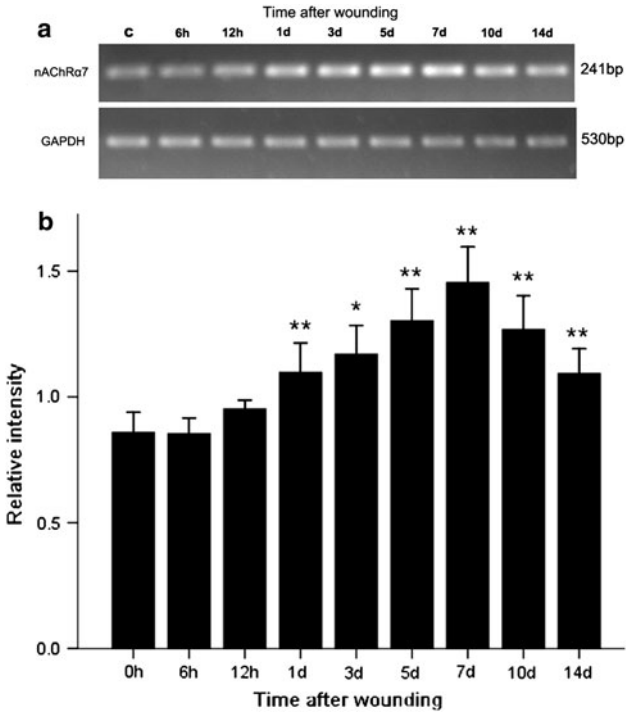

Fig. 9 **a** Analysis of nAChRα7 and GAPDH mRNA expressions from skin specimens by RT-PCR. *Lane C* represents the result of the control skin samples. Representative results from five individual animals are shown. **b** Relative intensity of nAChRα7 to GAPDH. All values represent the mean ± SD ($n = 5$). $^{**}P < 0.05$ (vs. control group and preceding group); $^{*}P < 0.05$ (vs. control group)

epidermis overlying the dermal fibrotic lesions is no longer considered solely as a protective barrier, because in epithelial–mesenchymal signaling pathway, keratinocytes contribute to normal and abnormal wound healing processes by releasing a broad spectrum of biologically active substances that modulate the activity of other epithelial cells as well as of dermal fibroblasts, endothelial cells, granulocytes and macrophages in a paracrine and autocrine manner (Bellemare et al. 2005; Funayama et al. 2003; Karrer et al. 2004; Mann et al. 2001; Ong et al. 2007; Shephard et al. 2004). Our results might reinforce the importance of epithelial–mesenchymal interaction in skin wound healing, which is also involved in the effects of non-neuronal ACh or choline mediated by nAChRα7.

In conclusion, we present an extensive distribution and time-dependent expression of nAChRα7 in multiple cell types during skin wound healing in mice. Our results indicate the significance of this specific nicotinic receptor subunit and the non-neuronal cholinergic system in skin wound healing, which may provide implications for the development of new strategies directed at the regulation of the cholinergic and nAChRα7-mediated mechanisms.

Acknowledgments This study was financially supported in part by grants from the Research Fund for the Doctoral Program funded by the Ministry of Education of China (200801590020) and National Natural Science Foundation of China (30271347).

References

Abe R, Donnelly SC, Peng T, Bucala R, Metz CN (2001) Peripheral blood fibrocytes: differentiation pathway and migration to wound sites. J Immunol 166:7556–7562

Aiba S, Tagami H (1997) Inverse correlation between CD34 expression and proline-4-hydroxylase immunoreactivity on spindle cells noted in hypertrophic scars and keloids. J Cutan Pathol 24:65–69

Alkondon M, Albuquerque EX (2004) The nicotinic acetylcholine receptor subtypes and their function in the hippocampus and cerebral cortex. Prog Brain Res 145:109–120

Alkondon M, Pereira EF, Cortes WS, Maelicke A, Albuquerque EX (1997) Choline is a selective agonist of alpha7 nicotinic acetylcholine receptors in the rat brain neurons. Eur J Neurosci 9:2734–2742

Anderson AA, Ushakov DS, Ferenczi MA, Mori R, Martin P, Saffell JL (2008) Morphoregulation by acetylcholinesterase in fibroblasts and astrocytes. J Cell Physiol 215:82–100

Andersson-Sjöland A, de Alba CG, Nihlberg K, Becerril C, Ramírez R, Pardo A, Westergren-Thorsson G, Selman M (2008)

Fibrocytes are a potential source of lung fibroblasts in idiopathic pulmonary fibrosis. Int J Biochem Cell Biol 40:2129–2140

Arredondo J, Nguyen VT, Chernyavsky AI, Bercovich D, Orr-Urtreger A, Kummer W, Lips K, Vetter DE, Grando SA (2002) Central role of alpha7 nicotinic receptor in differentiation of the stratified squamous epithelium. J Cell Biol 159:325–336

Arredondo J, Nguyen VT, Chernyavsky AI, Bercovich D, Orr-Urtreger A, Vetter DE, Grando SA (2003) Functional role of alpha7 nicotinic receptor in physiological control of cutaneous homeostasis. Life Sci 72:2063–2067

Bandapalli OR, Geheeb M, Kobelt D, Kuehnle K, Elezkurtaj S, Herrmann J, Gressner AM, Weiskirchen R, Beule D, Blüthgen N, Herzel H, Franke C, Brand K (2006) Global analysis of host tissue gene expression in the invasive front of colorectal liver metastases. Int J Cancer 118:74–89

Baum CL, Arpey CJ (2005) Normal cutaneous wound healing: clinical correlation with cellular and molecular events. Dermatol Surg 31:674–686

Bellemare J, Roberge CJ, Bergeron D, Lopez-Vallé CA, Roy M, Moulin VJ (2005) Epidermis promotes dermal fibrosis: role in the pathogenesis of hypertrophic scars. J Pathol 206:1–8

Bellini A, Mattoli S (2007) The role of the fibrocyte, a bone marrow-derived mesenchymal progenitor, in reactive and reparative fibroses. Lab Invest 87:858–870

Bucala R, Spiegel LA, Chesney J, Hogan M, Cerami A (1994) Circulating fibrocytes define a new leukocyte subpopulation that mediates tissue repair. Mol Med 1:71–81

Chernyavsky AI, Arredondo J, Marubio LM, Grando SA (2004) Differential regulation of keratinocyte chemokinesis and chemotaxis through distinct nicotinic receptor subtypes. J Cell Sci 117:5665–5679

Chesney J, Metz C, Stavitsky AB, Bacher M, Bucala R (1998) Regulated production of type I collagen and inflammatory cytokines by peripheral blood fibrocytes. J Immunol 160:419–425

Choi YH, Burdick MD, Strieter RM (2010) Human circulating fibrocytes have the capacity to differentiate osteoblasts and chondrocytes. Int J Biochem Cell Biol 42:662–671

Cooke JP (2007) Angiogenesis and the role of the endothelial nicotinic acetylcholine receptor. Life Sci 80:2347–2351

Flaherty M, Chojkier M (1986) Selective inhibition of collagen synthesis by the Ca2+ ionophore A23187 in cultured human fibroblasts. J Biol Chem 261:12060–12065

Follonier Castella L, Gabbiani G, McCulloch CA, Hinz B (2010) Regulation of myofibroblast activities: calcium pulls some strings behind the scene. Exp Cell Res 316:2390–2401

Funayama E, Chodon T, Oyama A, Sugihara T (2003) Keratinocytes promote proliferation and inhibit apoptosis of the underlying fibroblasts: an important role in the pathogenesis of keloid. J Invest Dermatol 121:1326–1331

Gahring LC, Rogers SW (2006) Neuronal nicotinic acetylcholine receptor expression and function on nonneuronal cells. AAPS J 7:E885–E894

Gomperts BN, Strieter RM (2007) Fibrocytes in lung disease. J Leukoc Biol 82:449–456

Grando SA (1997) Biological functions of keratinocyte cholinergic receptors. J Invest Dermatol Symp Proc 2:41–48

Grando SA, Kist DA, Qi M, Dahl MV (1993) Human keratinocytes synthesize, secrete, and degrade acetylcholine. J Invest Dermatol 101:32–36

Grando SA, Horton RM, Pereira EF, Diethelm-Okita BM, George PM, Albuquerque EX, Conti-Fine BM (1995) A nicotinic acetylcholine receptor regulating cell adhesion and motility is expressed in human keratinocytes. J Invest Dermatol 105:774–781

Guan DW, Ohshima T, Kondo T (2000) Immunohistochemical study on Fas and Fas ligand in skin wound healing. Histochem J 32:85–91

Hashimoto N, Jin H, Liu T, Chensue SW, Phan SH (2004) Bone marrow derived progenitor cells in pulmonary fibrosis. J Clin Invest 113:243–252

Herber DL, Severance EG, Cuevas J, Morgan D, Gordon MN (2004) Biochemical and histochemical evidence of nonspecific binding of alpha7nAChR antibodies to mouse brain tissue. J Histochem Cytochem 52:1367–1376

Hogg RC, Raggenbass M, Bertrand D (2003) Nicotinic acetylcholine receptors: from structure to brain function. Rev Physiol Biochem Pharmacol 147:1–46

Hong KM, Burdick MD, Phillips RJ, Heber D, Strieter RM (2005) Characterization of human fibrocytes as circulating adipocyte progenitors and the formation of human adipose tissue in SCID mice. FASEB J 19:2029–2031

Karlin A (2002) Emerging structure of the nicotinic acetylcholine receptors. Nat Rev Neurosci 3:102–114

Karrer S, Bosserhoff AK, Weiderer P, Landthaler M, Szeimies RM (2004) Keratinocyte-derived cytokines after photodynamic therapy and their paracrine induction of matrix metalloproteinases in fibroblasts. Br J Dermatol 151:776–783

Kawashima K, Fujii T (2008) Basic and clinical aspects of non-neuronal acetylcholine: overview of non-neuronal cholinergic systems and their biological significance. J Pharmacol Sci 106:167–173

Klapproth H, Reinheimer T, Metzen J, Munch M, Bittinger F, Kirkpatrick CJ, Hohle KD, Schemann M, Racke K, Wessler I (1997) Non-neuronal acetylcholine, a signalling molecule synthesized by surface cells of rat and man. Naunyn-Schmiedebergs Arch Pharmacol 355:515–523

Kummer W, Lips KS, Pfeil U (2008) The epithelial cholinergic system of the airways. Histochem Cell Biol 130:219–234

Kurzen H, Wessler I, Kirkpatrick CJ, Kawashima K, Grando SA (2007) The non-neuronal cholinergic system of human skin. Horm Metab Res 39:125–135

Liu RH, Mizuta M, Matsukura S (2004) The expression and functional role of nicotinic acetylcholine receptors in rat adipocytes. J Pharmacol Exp Ther 310:52–58

Mann A, Breuhahn K, Schirmacher P, Blessing M (2001) Keratinocyte-derived granulocyte-macrophage colony stimulating factor accelerates wound healing: stimulation of keratinocyte proliferation, granulation tissue formation, and vascularization. J Invest Dermatol 117:1382–1390

Metz CN (2003) Fibrocytes: a unique cell population implicated in wound healing. Cell Mol Life Sci 60:1342–1350

Metz CN, Tracey KJ (2005) It takes nerve to dampen inflammation. Nat Immunol 6:756–757

Mielke JG, Mealing GA (2009) Cellular distribution of the nicotinic acetylcholine receptor alpha7 subunit in rat hippocampus. Neurosci Res 65:296–306

Misery L (2004) Nicotine effects on skin: are they positive or negative? Exp Dermatol 13:665–670

Moore BB, Kolodsick JE, Thannickal VJ, Cooke K, Moore TA, Hogaboam C, Wilke CA, Toews GB (2005) CCR2-mediated recruitment of fibrocytes to the alveolar space after fibrotic injury. Am J Pathol 166:675–684

Mori L, Bellini A, Stacey MA, Schmidt M, Mattoli S (2005) Fibrocytes contribute to the myofibroblast population in wounded skin and originate from the bone marrow. Exp Cell Res 304:81–90

Moser N, Mechawar N, Jones I, Gochberg-Sarver A, Orr-Urtreger A, Plomann M, Salas R, Molles B, Marubio L, Roth U, Maskos U, Winzer-Serhan U, Bourgeois JP, Le Sourd AM, De Biasi M, Schröder H, Lindstrom J, Maelicke A, Changeux JP, Wevers A (2007) Evaluating the suitability of nicotinic acetylcholine receptor antibodies for standard immunodetection procedures. J Neurochem 102:479–492

Neumann S, Razen M, Habermehl P, Meyer CU, Zepp F, Kirkpatrick CJ, Wessler I (2007) The non-neuronal cholinergic system in peripheral blood cells: effects of nicotinic and muscarinic receptor antagonists on phagocytosis, respiratory burst and migration. Life Sci 80:2361–2364

Ong CT, Khoo YT, Tan EK, Mukhopadhyay A, Do DV, Han HC, Lim IJ, Phan TT (2007) Epithelial–mesenchymal interactions in keloid pathogenesis modulate vascular endothelial growth factor expression and secretion. J Pathol 211:95–108

Orr-Urtreger A, Göldner FM, Saeki M, Lorenzo I, Goldberg L, De Biasi M, Dani JA, Patrick JW, Beaudet AL (1997) Mice deficient in the alpha7 neuronal nicotinic acetylcholine receptor lack alpha-bungarotoxin binding sites and hippocampal fast nicotinic currents. J Neurosci 17:9165–9171

Osborne-Hereford AV, Rogers SW, Gahring LC (2008) Neuronal nicotinic alpha7 receptors modulate inflammatory cytokine production in the skin following ultraviolet radiation. J Neuroimmunol 193:130–139

Papke RL, Bencherif M, Lippiello P (1996) An evaluation of neuronal nicotinic acetylcholine receptor activation by quaternary nitrogen compounds indicates that choline is selective for the alpha 7 subtype. Neurosci Lett 213:201–204

Phillips RJ, Burdick MD, Hong K, Lutz MA, Murray LA, Xue YY, Belperio JA, Keane MP, Strieter RM (2004) Circulating fibrocytes traffic to the lungs in response to CXCL12 and mediate fibrosis. J Clin Invest 114:438–446

Quan TE, Cowper S, Wu SP, Bockenstedt LK, Bucala R (2004) Circulating fibrocytes: collagen-secreting cells of the peripheral blood. Int J Biochem Cell Biol 36:598–606

Rehan VK, Wang Y, Sugano S, Romero S, Chen X, Santos J, Khazanchi A, Torday JS (2005) Mechanism of nicotine-induced pulmonary fibroblast transdifferentiation. Am J Physiol Lung Cell Mol Physiol 289:L667–L676

Sakai N, Wada T, Yokoyama H, Lipp M, Ueha S, Matsushima K, Kaneko S (2006) Secondary lymphoid tissue chemokine (SLC/CCL21)/CCR7 signaling regulates fibrocytes in renal fibrosis. Proc Natl Acad Sci USA 103:14098–14103

Schmidt M, Sun G, Stacey MA, Mori L, Mattoli S (2003) Identification of circulating fibrocytes as precursors of bronchial myofibroblasts in asthma. J Immunol 171:380–389

Sekhon HS, Keller JA, Proskocil BJ, Martin EL, Spindel ER (2002) Maternal nicotine exposure upregulates collagen gene expression in fetal monkey lung. Association with alpha7 nicotinic acetylcholine receptors. Am J Respir Cell Mol Biol 26:31–41

Shephard P, Martin G, Smola-Hess S, Brunner G, Krieg T, Smola H (2004) Myofibroblast differentiation is induced in keratinocyte-fibroblast co-cultures and is antagonistically regulated by endogenous transforming growth factor-beta and interleukin-1. Am J Pathol 164:2055–2066

Su X, Lee JW, Matthay ZA, Mednick G, Uchida T, Fang X, Gupta N, Matthay MA (2007) Activation of the alpha7 nAChR reduces acid-induced acute lung injury in mice and rats. Am J Respir Cell Mol Biol 37:186–192

Tracey KJ (2002) The inflammatory reflex. Nature 420:853–859

Wang H, Yu M, Ochani M, Amella CA, Tanovic M, Susarla S, Li JH, Wang H, Yang H, Ulloa L, Al-Abed Y, Czura CJ, Tracey KJ (2003) Nicotinic acetylcholine receptor alpha7 subunit is an essential regulator of inflammation. Nature 421:384–388

Werner S, Grose R (2003) Regulation of wound healing by growth factors and cytokines. Physiol Rev 83:835–870

Xiu J, Nordberg A, Zhang JT, Guan ZZ (2005) Expression of nicotinic receptors on primary cultures of rat astrocytes and up-regulation of the alpha7, alpha4 and beta2 subunits in response to nanomolar concentrations of the beta-amyloid peptide(1–42). Neurochem Int 47:281–290

Yang L, Scott PG, Dodd C, Medina A, Jiao H, Shankowsky HA, Ghahary A, Tredget EE (2005) Identification of fibrocytes in postburn hypertrophic scar. Wound Repair Regen 13:398–404

Yu TS, Cheng ZH, Li LQ, Zhao R, Fan YY, Du Y, Ma WX, Guan DW (2010) The cannabinoid receptor type 2 is time-dependently expressed during skeletal muscle wound healing in rats. Int J Legal Med 124:397–404

Zia S, Ndoye A, Lee TX, Webber RJ, Grando SA (2000) Receptor mediated inhibition of keratinocyte migration by nicotine involves modulations of calcium influx and intracellular concentration. J Pharmacol Exp Ther 293:973–981